Seasonal forcing and waning immunity drive the sub-annual periodicity of the COVID-19 epidemic

Ilan N. Rubin[1*], Mary Bushman[1], Marc Lipsitch[1], William P. Hanage[1]

[1]Epidemiology, Harvard T.H. Chan School of Public Health, Boston & 02115, United States.

[*]Corresponding author. Email: ilan.n.rubin@gmail.com

Seasonal trends in infectious diseases are shaped by climatic and social factors, with many respiratory viruses peaking in winter. However, the seasonality of COVID-19 remains in dispute, with significant waves of cases across the United States occurring in both winter and summer. Using wavelet analysis of COVID-19 cases, we find that the periodicity of epidemic COVID-19 varies markedly across the U.S. and correlates with winter temperatures, indicating seasonal forcing. However, the pattern of multiple waves per year that has been so disruptive and unique to COVID-19 cannot be explained by seasonal forcing. Using a modified SIRS model that allows specification of the tempo of waning immunity, we show that specific forms of non-durable immunity can sufficiently explain the sub-annual waves characteristic of the COVID-19 epidemic.

Introduction

Many infectious diseases show pronounced seasonal patterns, producing waves of cases at particular times each year. Such seasonality is important for practical purposes in public health, allowing improved forecasting of heightened healthcare demand. Agents that transmit via the respiratory route are typically associated with a peak in the winter months, for reasons that may be due to climatic conditions and/or changing contact patterns during that period. In the case of the COVID-19 epidemic, waves of transmission occur not only in the winter, but also often occurred during the spring or summer, and have thus been out of sync with the classical pattern of respiratory viral pathogens. Untangling the seasonality of the COVID-19 epidemic from patterns in viral evolution, patterns in population immunity, and epidemic stochasticity is a difficult yet imperative, task.

In the case of a pandemic virus for which levels of immunity in the population are initially low, seasonality is difficult to determine because the large proportion of susceptible individuals allow commensurately large surges of infections even at times of year when this would not be expected in the presence of significant immunity following the pandemic period (*1*).

In the United States, multiple waves of infection have been documented each year since the end of 2019. Epidemic severity has tended to alternate between the northern and southern United States with evidence for a strong summer wave in the southern United States (*2*) as well as a negative temporal correlation between the number of cases and absolute humidity (*3*). Despite this periodic regularity, the precise patterns of seasonality, and thus their predictability going forward, remain to be determined.

While changes in case ascertainment make it hard to determine absolute incidence in the absence of large-scale community surveys (such as (*4*)), wavelet analysis offers an alternative approach to assess changing periodicity. Wavelet analysis is a spectral decomposition method similar to continuous Fourier transformation that is also able to handle non-stationary time series data. This approach is useful in the pandemic context because it does not assume a single fixed periodicity and can therefore determine whether the oscillatory characteristic of the epidemic changes over time (*5*). For example, Grenfell et al. showed how the periodicity of measles cases in London changed after the onset of vaccination (*6*). Similar analyses of the COVID-19 epidemic for various countries around the world (*7, 8*), have as yet analyzed the very early part of the epidemic where only

one or two epidemic waves had taken place and therefore offer limited insight into the long-term trajectory of the disease.

The United States offers a useful case study for how climate effects epidemic seasonality, having a range of very different climates together with readily available and high-quality estimates of case counts. Here we use wavelet analysis to determine the periodicity of COVID-19 waves in the United States using county level COVID-19 case estimates and determine how periodicity is correlated with measures of mobility, climatic, and demographic variables.

COVID-19 displays both annual and sub-annual periodic signals

We applied wavelet decomposition to the logarithm of the 7-day rolling averages of cases per 100,000 individuals as compiled by the New York Times from January 21, 2020 through March 24, 2023, the entirety of the time they were reported (*9*). The global wavelet spectrum, which is calculated by averaging the wavelets over the entire time period and is analogous to a Fourier spectrum, is a simple characterization of the periodicity of COVID-19 cases over that time period and shows the distribution periodic components that make up the time series of COVID-19 cases [see fig. S1 for examples of full wavelets].

The state-level global wavelet spectra are relatively consistent across U.S. states and territories and generally show two major components [Fig. 1]. The first has a period of approximately 365 days, as one would expect for a disease with classical winter waves of infections. The second major component is sub-annual and generally peaks between 120 and 180 days depending on the state and is consistent with the pattern of multiple large waves of transmission that occurred each year from 2020-2023 for most of the United States.

COVID-19 periodicity is correlated to temperature

Strikingly, states with warmer winters (as quantified here by the average over 2020 to 2023 of the lowest of the monthly minimum temperature each year according to NOAA's Monthly U.S. Climate Divisional Database (*10*)) were dominated by the sub-annual component and display little, if any, annual seasonality [Fig. 1]. Conversely, states with colder winter low temperatures have annual and sub-annual components of similar magnitude in their global wavelet spectra and display a

comparatively larger annual signal than more tropical states. Further supporting this pattern, of the four states and territories (Alaska, Hawaii, Puerto Rico, and the Virgin Islands – shown in grey) that are not included in the NOAA Climate Divisional Database, three have very tropical climates and show essentially no signature of annual periodicity, while Alaska has a larger annual component. This difference in epidemic periodicity can be seen in the case counts as Florida, Louisiana, and Georgia (the states with the most tropical climates) experienced two relatively similarly sized waves a year, while Minnesota, North Dakota, and South Dakota (the states with the coldest climates) experienced a large winter wave each of the three years with no or much smaller off-peak waves [fig. S4].

We extend this analysis to the county level and quantify the strength of the annual component as the power of the global wavelet spectrum at a period of 365 days. While this quantification is a relatively simple description of the seasonality of the epidemic in each county, it provides an intuitive way to summarize, in a single number, how strong the annual-scale periodicity of COVID-19 across the United States. In doing so, a clear pattern emerges. Counties in the southern and western United States, and particularly the southeast, show little annual periodicity, while counties in the Midwest and northeast of the United States experienced much more annual epidemics [Fig. 1]. Counties around the Rocky Mountains have a less distinct pattern yet are also often less populous and therefore likely more dominated by stochastic dynamics.

In concert with this visually apparent trend [Fig. 1], the power of the annual component for the COVID-19 epidemic across U.S. counties is significantly negatively correlated to temperature minimums (as defined by the average over 2020-2023 of the lowest monthly minimum temperature each year in the NOAA's Climate Divisional Database (*10*)) across U.S. counties [Table 1]. Counties with colder winters) were more likely to have experienced strongly annual COVID-19 epidemics, while counties with tropical climates (or those with warmer winter temperatures) were more likely to have epidemics dominated by sub-annual waves.

The maximum temperature of the county is also negatively correlated (to a lesser degree) with the strength of the annual component, a further link between colder climates and strongly annual COVID-19 epidemic dynamics. However, temperature variability (as defined by the difference between summer high and winter low temperatures) is positively correlated, possibly indicating that an annual epidemic cycle is associated with the overall extremity of the regional climate as

well, rather than simple cold winters. Previous work on early pandemic dynamics has indicated higher transmission rates during the winter through direct correlations of cold temperatures with case counts (*3, 11*) and that the SARS-CoV-2 virus degrades more slowly in low temperatures and extreme relative humidity (*12*), a possible mechanism driving this periodic variability. However, the small a negative correlation with high temperatures in the summer may indicate that an annual epidemic cycle is associated with the overall extremity of the regional climate, rather than simply the cold winters.

In contrast with temperature, most socio-demographic characteristics of the county had little to no effect. Population size, population density, elderly population, geographic area of the county, and the political leaning of the county show little correlation to the COVID-19 epidemic periodicity [Table 1, fig. S6]. Thus, while the political partisanship of a county is known to be significantly correlated with the magnitude of the epidemic in that county (*13*), the timing of their waves was seemingly unaffected. We also, conducted similar wavelet analyses of Google mobility data (specifically their "retail and recreation" and "workplace" variables), that is both visually and intuitively periodic on an annual cycle (people move around more in the summer than winter). However, the mobility of the population explained under 3% of the variation in epidemic periodicity, compared to the more than 20% that is explained by temperature seasonality.

Other variables that show relatively high correlation with the annual periodicity of the epidemic may be explained by their association with climate. For instance, of the ten Health and Human Services regions, the region of states around the Great Lakes (Region 5) has a significantly higher level of annual periodicity [fig. S6], a pattern that is consistent with temperature minimum. Similarly, the correlation with the percentage of the population with health insurance can be largely explained by low rates of insurance in Texas and Florida [Fig. S5], two states with comparatively tropical climates. A multivariable regression shows that the annual component is associated the minimum but not maximum temperatures in a location, further emphasizing the role of cold weather in predicting stronger annual cycles [table S1].

While this work cannot establish the precise mechanisms underlying the periodicity we observe, we note that the regular timing of the winter peak each year [fig. S3] is consistent with the winter holiday period even in places with little evidence of an annual component (e.g., Florida) [fig. S4] and perhaps consistent with the increased mixing and changing contact patterns over the holiday

period. However, holiday travel is relatively consistent across the U.S., yet COVID-19 periodicity is not and is instead correlated to temperature, supporting the possible climatic mechanism to seasonal forcing. Further comparisons with other regions around the world with different holiday schedules and climate variability may provide further evidence for this proposition. Most importantly, the marked dose-response relationship between climatic variability and annual periodicity is a strong indication that the observed periodicity is not simply due to chance arrivals of new SARS-CoV-2 strains at approximately annual intervals, and instead suggests that some climate-related drivers (including behavioral consequences) are an important driver of annual seasonality.

Individual waning immunity as a model of sub-annual periodicity

While the previously described wave decomposition analyses provided insight and intuition into the character of the periodicity of the COVID-19 epidemic, these analyses are non-mechanistic. Previous theory on seasonal forcing shows how epidemics can be forced into an annual cycle or longer multiennial cycles (*6, 14, 15*). For instance, Dushoff et al. show how undetectably small changes in transmission rate over the course of an annual cycle can result in large oscillations in influenza incidence through dynamical resonance of the disease and seasonal dynamics (*16*). However, this seasonal forcing theory largely pertains to epidemics with annual or longer cycles.

The classical SIRS model (Susceptible-Infectious-Recovered-Susceptible) can drive waves in the number of infected individuals through cycles of the depletion and replenishment of the number of susceptibles as immunity in the population wanes. However, the classical SIRS model does not consider partial or waning immunity, but absolute immunity that wanes immediately (with the time persons are immune distributed exponentially in the population) (*17*). Under these classical assumptions, while the inter-epidemic period can be controlled as a function of the average length of time an individual is immune, epidemic waves are always damped oscillations (decrease in size from one wave to the next) and are thus not maintained over long periods (*18*). To provide intuition into possible mechanisms that could be driving this more unusual sustained sub-annual periodic behavior, we introduce a generalization of the classic SIRS epidemic model that includes both partial immunity that wanes over the time since recovery as well as seasonal forcing [Fig. 2].

The model can be described as a system of partial differential equations with Susceptible (S),

infectious (I), and Recovered (R) classes that are a function of time (t) and time since recovery from infectiousness (a). Individuals can become infected from both the Susceptible and Recovered classes with immunity from infection for the Recovered class described by a function $\omega(a)$. While this function can take any form, here we use a functional form based on the cumulative distribution function for a Weibull distribution that allows for easy tuning between exponentially and more stepwise (sigmoidal) decaying immune waning functions [e.g., see Fig. 2 and fig. S7]. The model is as follows:

$$\frac{S(t)}{dt} = -\beta(t)I(t)S(t) \tag{1}$$

$$\frac{dI(t)}{dt} = \beta(t)I(t)\left(S(t) + \int_0^\infty R(t,a)\omega(a)\ da\right) - \gamma I(t) \tag{2}$$

$$\frac{\partial R(t,a)}{\partial t} + \frac{\partial R(t,a)}{\partial a} = -\beta(t)I(t)R(t,a)\omega(a) \tag{3}$$

with the following boundary condition:

$$R(t,0) = \gamma I(t) \tag{4}$$

and the following waning immunity function:

$$\omega(a \mid k, \lambda, \omega_\infty) = exp\left(-\left(\frac{a}{\lambda}log(2)^{1/k}\right)^k\right)(1-\omega_\infty) + \omega_\infty \tag{5}$$

where γ represents the recovery rate from the infected to the recovered (aka immune) class and $\beta(t)$ is the transmission rate at time t (*19*). The immunity waning function is governed by three parameters: k is the shape parameter that controls the steepness of the waning, λ represents the "half-life" and controls the timing, and ω_∞ is the asymptote or amount of immunity maintained for perpetuity. For a more detailed discussion of the model including the sinusoidal seasonal forcing function, see material and methods.

For computational simplicity, we simulated an individual-based version of the SIR model with waning immunity and seasonal forcing. We ran 125,000 simulations using Latin hypercube sampling (*20*) to sample the three immune waning parameters with different amounts of annual seasonal forcing as part of the transmission rate. The simulations were then analyzed based on the number of epidemic waves (determined numerically from the stochastic simulations, see the material and methods for more details) that occur per year of the simulation in order to understand which

immunity regimes generate sub-annual epidemic periodicity that is maintained over a relatively long period of time (i.e., effectively undamped oscillations) with and without seasonal forcing.

The model is able to produce sub-annual waves when three conditions are met: there is little long-term immunity ($\omega_\infty < 0.5$, immunity wanes relatively sharply ($k > 1.5$), and half-life time of immunity is short ($\lambda < 200$ days) [fig. S7]. In practical terms, this represents waning functions that have a sigmoidal shape and thus a period of strong immunity, a transition period with partial immunity that occurs with about half a year or less, and very little immunity in the long-term. This durability is roughly in line with epidemiological estimates of the durability of immunity to SARS-CoV-2 (*21–23*).

In general, the shape parameter of the waning function (k) and the amount of long-term immunity (ω_∞) determine whether stable periodicity is possible, while the frequency of that periodicity is largely a function of the half-life of the immunity (λ). For example simulation trajectories and immune waning functions, see figure S7.

Perhaps most importantly, including annual seasonal forcing on the transmission rate had little to no effect on the generation of sub-annual periodicity and instead only increased the likelihood of annual waves [fig. 3]. Thus, while seasonal forcing undoubtedly would impact the magnitude and timing of the epidemic waves [for example trajectories with seasonal forcing see fig. S8], likely in a chaotic way due to the resonance and synchrony of the two processes (*24, 25*), it is unlikely to change the importance of non-durable immunity in generating such rapidly reoccurring epidemic waves.

While the evolution of the SARS-CoV-2 virus has unarguably played a large role in the magnitude and duration of each wave of infections, the regular timing of the waves implies that a more deterministic mechanism (such as immune dynamics or seasonal forcing) has been a necessary driver of the periodic dynamics. While previous work finds that short-duration infections, continuous antigenic drift, and complete cross-immunity between strains can generate periodic waves of infections (*26*), here we show short-term immunity that wanes quickly is a sufficient condition for regular sub-annual periodicity, independent of multi-strain dynamics.

Moreover, antigenic evolution effectively accelerates the rate with which the immunity of the population wanes as replacing strains outcompete their predecessors and so the continued antigenic evolution of the virus has a similar effect to a sharply declining waning immunity function. An

individual's "effective immunity" does not only consider their individual immune response, but also the whether the individual immune response is well matched to the virus that is circulating at that time. Previous work has examined when the repeated turnover or coexistence of viral strains occurs within existing periodic dynamics (*27, 28*) and provides an example of how continued theoretical work understanding how large-scale evolutionary change in viral antigens – such as that which occurred in the BA.1, BA.2, and BA.2.86 variants (*29, 30*) – interacts with the sub-annual periodic dynamics described here.

Waning immunity at the level of individuals will occur in the context of the antigenic drift and strain replacement that has been observed and likely will continue to occur (*31, 32*). This model allows the short-term and imperfect immunity following COVID-19 infection to be incorporated in a simple yet flexible way which reproduces the near-deterministic sub-annual periodicity we have also described.

Conclusions

While the patterns reported in this work have been consistent throughout the study period, the accumulation and loss of immunity, unforeseeable viral evolution, and unpredictable nature of complex and possibly chaotic wave dynamics make detailed forecasting a challenge. While some have postulated that COVID-19 will inevitably transition to annual winter waves (*33*) that are a classical characteristic of other respiratory viral pathogens in the endemic state (*14, 16, 33–35*), we have shown here that this transition has yet to take place, though annual waves are a key part of the dynamics, especially in colder climates. Continued surveillance will be essential to monitor if these dynamics have stabilized into a predictable cycle or continue to evolve yet changes in case reporting as the immediate threat of the pandemic has dwindled means that mild cases are likely to remain under-counted and present a challenge. While wastewater surveillance emerged during the pandemic as a new means to track disease trends in close to real time (*36, 37*), it has not been universally applied and has remaining theoretical challenges as a direct replacement for high-quality estimates of disease incidence. Nevertheless, wastewater surveillance data collected from diverse regions going forward may provide early indication if the patterns observed here remain stable in the post-pandemic.

We have shown evidence for distinct patterns of seasonality in COVID-19 cases across the U.S., correlated with climate. In regions with colder winters, an annual component predominates, while in warmer regions circulation throughout the year is marked by multiple sub-annual waves occurring every 3-4 months. We also show that annual seasonal forcing is unable alone explain these sub-annual waves but instead must work in concert with another periodic generating mechanism such as the steeply waning, short-term convalescent immunity proposed here. Although we are not able to disentangle how viral evolution combines with the waning human immune response in producing such conditions, the functional result remains the same. Improved understanding of how seasonal forcing and viral evolution interact with quickly waning immunity will permit future extensions of the classical SIRS model to describe other periodic epidemics.

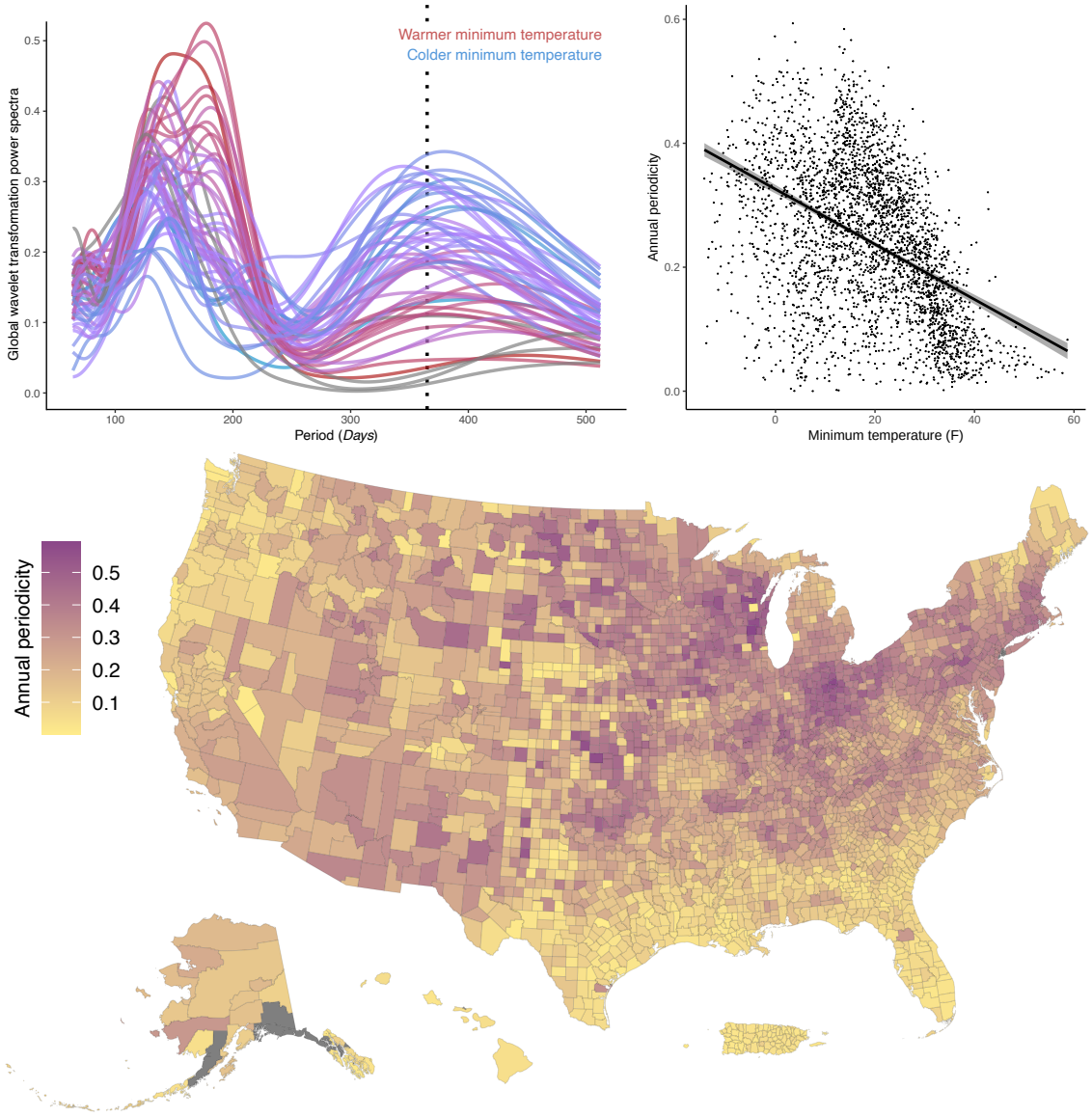

Figure 1: **COVID-19 periodicity across the United States.** Wavelet transformations were calculated for log of COVID-19 incidence for each U.S. state, Puerto Rico and the Virgin Islands. (**A**) Curves are colored by the minimum of the state-wide average monthly low temperature measured between 2020 and 2023. States with a warmer winter temperature are shown in red and cooler states in blue. Areas not included in NOAA's historical climate dataset (Alaska, Hawaii, Puerto Rico, and the Virgin Islands) are shown in grey. A dashed line is shown at 365 days. (**B**) COVID-19 annual component as a function of temperature seasonality for each county in the United States. The magnitude of the annual component was calculated as the power of the global wavelet spectrum at 365 days. (**C**) A map of all counties in the United States colored by the magnitude of their annual component.

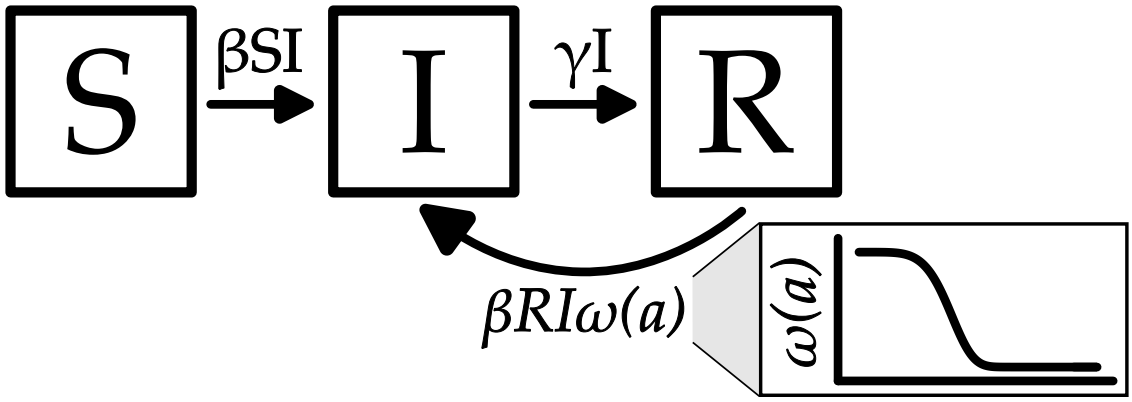

Figure 2: **SIR model with waning immunity compartment diagram.** A representation of the proposed SIR model with waning immunity. S, I, and R represent the susceptible, infected, and recovered states respectively and are all functions of time, t. β is the transmission rate and may be either a static variable or a function of time, t, while γ is the rate of recovery from illness. In the classical SIRS model, recovered individuals lose all immunity and return to the susceptible compartment after some time. In the model presented, individuals remain "recovered" for perpetuity but over time can be reinfected as a function of waning immunity $\omega(a)$, where a is the time since recovery. In this model S represents an initial state made up of individuals who have never been infected and have no immunity.

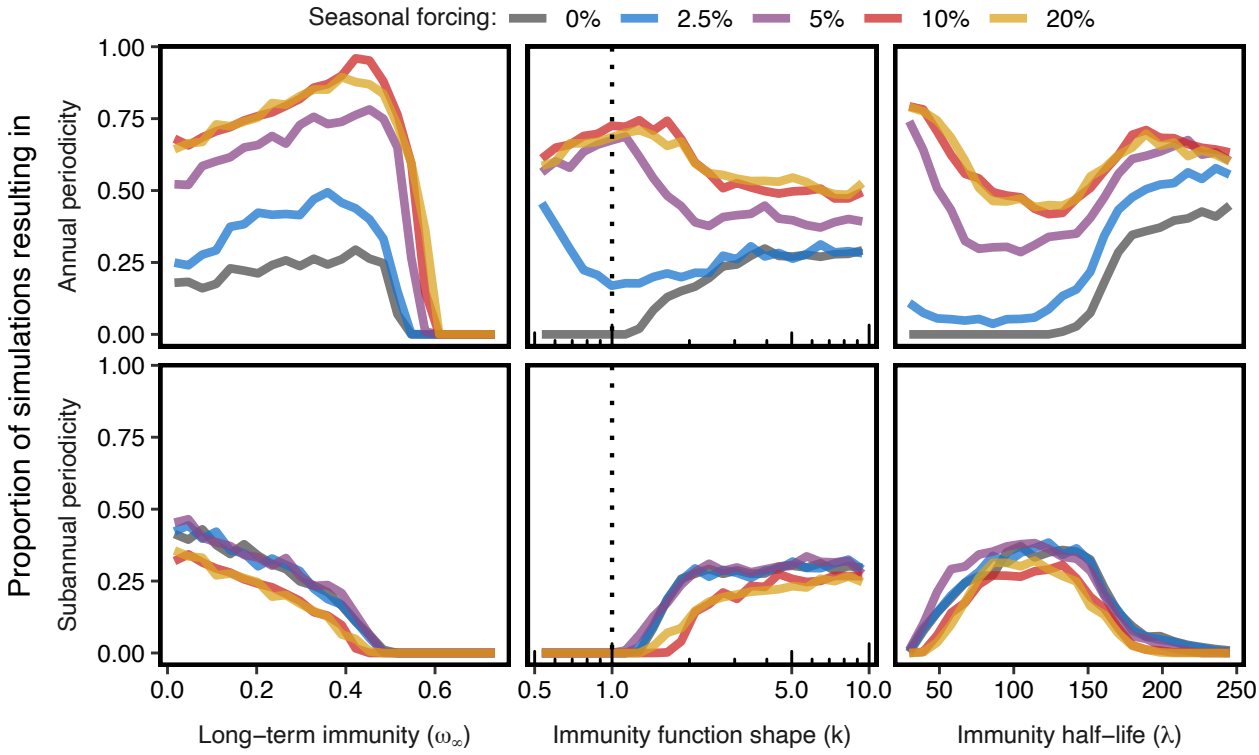

Figure 3: **Seasonal forcing does not markedly affect sub-annual periodicity in simulated epidemics.** We ran 125,000 simulations of the individual-based implementation of the SIRS model with individually waning immunity, with 25,000 simulations for each of five different parameterizations of seasonal forcing (shown in color with $\theta = 2.5\%, 5\%, 10\%$, and 20%, or when the peak transmission rate is $\theta\%$ higher transmission than at its lowest). Immune parameters were chosen randomly with Latin Hypercube Sampling for each seasonality regime ($\omega_\infty \in (0, 0.75)$, $k \in (0.5, 10)$, and distributed logarithmically $\lambda \in (25, 250)$). Annual periodicity is defined as any simulation with an inter-epidemic period of between 9 and 18 months and sub-annual of less than 9 months, both requiring more than 5 total waves during the 10 simulation years to filter out strongly damped oscillations. Simulations that did not result in either annual or sub-annual waves either reached a stable equilibrium endemic state or resulted in waves less frequent than every 18 months. The probability of an annually reccurring epidemic generally increases with increasing seasonal forcing, dependent on the immunity characteristics. However, the presence of seasonal forcing has little to no effect on driving sub-annually reoccurring epidemics. The dashed lines represent exponentially waning immunity, a good proxy for the classic SIRS model, and where undamped sub-annual waves are never generated. For an epidemic to be periodic at all immunity must wane sharply ($k \gtrapprox 1.5$) and the long-term immunity must be marginal ($\omega_\infty \lessapprox 0.5$).

Table 1: **Correlations between COVID-19 annual component and various climatic and socio-demographic variables.** Wavelet analyses were calculated for the log of COVID-19 cases until March 2023 as estimated by the New York Times for each county (or county equivalent) in the United States. Regressions were calculated for the global wavelet transformation (average of the wavelet transformation over time) for a period of 365 days as a function of various climatic and socio-demographic variables. Positive slopes indicate that an increase in the variable in questions is correlated to an increase in the power of the annual component of COVID-19 in that county. Due to the large sample sizes, all correlations were statistically significant. Variables with $r^2 > 0.1$ are bolded.

Variable	Pearson's correlation	r^2	source
Minimum temperature	−0.400	**0.202**	(*10*)
Maximum temperature	−0.231	$5.06 \cdot 10^{-2}$	(*10*)
Difference of max and min temperature	0.331	**0.150**	(*10*)
Average monthly precipitation	−0.110	$2.74 \cdot 10^{-2}$	(*10*)
Log population size	0.196	$2.72 \cdot 10^{-2}$	(*38*)
% Population age 65+	−0.120	$7.12 \cdot 10^{-3}$	(*38*)
% Population under 200% of the poverty line	−0.281	$8.40 \cdot 10^{-2}$	(*38*)
% Population Insured	0.382	**0.149**	(*38*)
Log population density	0.147	$6.99 \cdot 10^{-3}$	(*38, 39*)
Log geographic area	$2.52 \cdot 10^{-2}$	$1.82 \cdot 10^{-3}$	(*39*)
Republican vote %, 2020 presidential election	$4.28 \cdot 10^{-2}$	$6.88 \cdot 10^{-3}$	(*40*)
Google mobility periodicity (retail)	0.169	$2.87 \cdot 10^{-2}$	(*41*)
Google mobility periodicity (workplace)	$-9.47 \cdot 10^{-2}$	$8.96 \cdot 10^{-3}$	(*41*)
Log total number of COVID-19 cases	0.197	$2.60 \cdot 10^{-2}$	(*9*)
HHS region (ANOVA)		**0.230**	(*41*)

References and Notes

1. J. Shaman, E. Goldstein, M. Lipsitch, Absolute Humidity and Pandemic Versus Epidemic Influenza. *American Journal of Epidemiology* **173** (2), 127–135 (2010), doi:10.1093/aje/kwq347.

2. H. Jalal, K. Lee, D. S. Burke, Oscillating spatiotemporal patterns of COVID-19 in the United States. *Scientific Reports* **14** (1) (2024), doi:10.1038/s41598-024-72517-6.

3. G. Lin, *et al.*, Investigating the effects of absolute humidity and movement on COVID-19 seasonality in the United States. *Scientific Reports* **12** (1) (2022), doi:10.1038/s41598-022-19898-8.

4. S. Riley, *et al.*, REal-time Assessment of Community Transmission (REACT) of SARS-CoV-2 virus: Study protocol. *Wellcome Open Research* **5**, 200 (2021), doi:10.12688/wellcomeopenres.16228.2.

5. B. Cazelles, M. Chavez, G. C. de Magny, J.-F. Guégan, S. Hales, Time-dependent spectral analysis of epidemiological time-series with wavelets. *Journal of The Royal Society Interface* **4** (15), 625–636 (2007), doi:10.1098/rsif.2007.0212.

6. B. T. Grenfell, O. N. Bjørnstad, J. Kappey, Travelling waves and spatial hierarchies in measles epidemics. *Nature* **414** (6865), 716–723 (2001), doi:10.1038/414716a.

7. G. Campi, A. Bianconi, Periodic recurrent waves of Covid-19 epidemics and vaccination campaign. *Chaos, Solitons, and Fractals* **160**, 112216 (2022), doi:10.1016/j.chaos.2022.112216.

8. G. Campi, A. Perali, A. Marcelli, A. Bianconi, Sars-Cov2 world pandemic recurrent waves controlled by variants evolution and vaccination campaign. *Scientific Reports* **12** (1) (2022), doi:10.1038/s41598-022-22816-7.

9. The New York Times, *Coronavirus (Covid-19) Data in the United States*, Tech. rep. (Accessed 2024), `https://github.com/nytimes/covid-19-data`.

10. R. S. Vose, *et al.*, NOAA's Climate Divisional Database (nCLIMDIV) (2014), doi:10.7289/V5M32STR.

11. J. Landier, *et al.*, Cold and dry winter conditions are associated with greater SARS-CoV-2 transmission at regional level in western countries during the first epidemic wave. *Scientific Reports* **11** (1) (2021), doi:10.1038/s41598-021-91798-9.

12. D. H. Morris, *et al.*, Mechanistic theory predicts the effects of temperature and humidity on inactivation of SARS-CoV-2 and other enveloped viruses. *eLife* **10** (2021), doi:10.7554/eLife.65902.

13. J. Kaashoek, *et al.*, The evolving roles of US political partisanship and social vulnerability in the COVID-19 pandemic from February 2020–February 2021. *PLOS Global Public Health* **2** (12), e0000557 (2022), doi:10.1371/journal.pgph.0000557.

14. J. Shaman, V. E. Pitzer, C. Viboud, B. T. Grenfell, M. Lipsitch, Absolute Humidity and the Seasonal Onset of Influenza in the Continental United States. *PLoS Biology* **8** (2), e1000316 (2010), doi:10.1371/journal.pbio.1000316.

15. R. E. Baker, W. Yang, G. A. Vecchi, C. J. E. Metcalf, B. T. Grenfell, Susceptible supply limits the role of climate in the early SARS-CoV-2 pandemic. *Science* **369** (6501), 315–319 (2020), doi:10.1126/science.abc2535.

16. J. Dushoff, J. B. Plotkin, S. A. Levin, D. J. D. Earn, Dynamical resonance can account for seasonality of influenza epidemics. *Proceedings of the National Academy of Sciences* **101** (48), 16915–16916 (2004), doi:10.1073/pnas.0407293101.

17. M. E. Khalifi, T. Britton, Extending susceptible-infectious-recovered-susceptible epidemics to allow for gradual waning of immunity. *Journal of The Royal Society Interface* **20** (206) (2023), doi:10.1098/rsif.2023.0042.

18. E. B. Wilson, J. Worcester, Damping of Epidemic Waves. *Proceedings of the National Academy of Sciences* **31** (9), 294–298 (1945), doi:10.1073/pnas.31.9.294.

19. Here modeled as a sinusoidal function: $\beta(t) = \beta_0(1 + \theta \cos((2t/365 + s_\theta)\pi))$.

20. M. D. McKay, R. J. Beckman, W. J. Conover, A Comparison of Three Methods for Selecting Values of Input Variables in the Analysis of Output from a Computer Code. *Technometrics* **21** (2), 239 (1979), doi:10.2307/1268522.

21. Y. Goldberg, *et al.*, Protection and Waning of Natural and Hybrid Immunity to SARS-CoV-2. *New England Journal of Medicine* **386** (23), 2201–2212 (2022), doi:10.1056/NEJMoa2118946.

22. C. Hernandez-Suarez, E. Murillo-Zamora, Waning immunity to SARS-CoV-2 following vaccination or infection. *Frontiers in Medicine* **9** (2022), doi:10.3389/fmed.2022.972083.

23. J. P. Townsend, H. B. Hassler, P. Sah, A. P. Galvani, A. Dornburg, The durability of natural infection and vaccine-induced immunity against future infection by SARS-CoV-2. *Proceedings of the National Academy of Sciences* **119** (31) (2022), doi:10.1073/pnas.2204336119.

24. S. Altizer, *et al.*, Seasonality and the dynamics of infectious diseases. *Ecology Letters* **9** (4), 467–484 (2006), doi:10.1111/j.1461-0248.2005.00879.x.

25. D. J. D. Earn, P. Rohani, B. M. Bolker, B. T. Grenfell, A Simple Model for Complex Dynamical Transitions in Epidemics. *Science* **287** (5453), 667–670 (2000), doi:10.1126/science.287.5453.667.

26. J. R. Gog, B. T. Grenfell, Dynamics and selection of many-strain pathogens. *Proceedings of the National Academy of Sciences* **99** (26), 17209–17214 (2002), doi:10.1073/pnas.252512799.

27. S. W. Park, S. Cobey, C. J. E. Metcalf, J. M. Levine, B. T. Grenfell, Predicting pathogen mutual invasibility and co-circulation. *Science* **386** (6718), 175–179 (2024), doi:10.1126/science.adq0072.

28. M. Bushman, R. Kahn, B. P. Taylor, M. Lipsitch, W. P. Hanage, Population impact of SARS-CoV-2 variants with enhanced transmissibility and/or partial immune escape. *Cell* **184** (26), 6229–6242.e18 (2021), doi:10.1016/j.cell.2021.11.026.

29. K. Khan, *et al.*, Evolution and neutralization escape of the SARS-CoV-2 BA.2.86 subvariant. *Nature Communications* **14** (1) (2023), doi:10.1038/s41467-023-43703-3.

30. J. Ai, *et al.*, Antibody evasion of SARS-CoV-2 Omicron BA.1, BA.1.1, BA.2, and BA.3 sublineages. *Cell Host &; Microbe* **30** (8), 1077–1083.e4 (2022), doi:10.1016/j.chom.2022.05.001.

31. M. Meijers, D. Ruchnewitz, J. Eberhardt, M. Luksza, M. Lässig, Population immunity predicts evolutionary trajectories of SARS-CoV-2. *Cell* **186** (23), 5151–5164.e13 (2023), doi:10.1016/j.cell.2023.09.022.

32. J. J. Bull, K. Koelle, R. Antia, Waning immunity drives respiratory virus evolution and reinfection. *Evolution, Medicine, and Public Health* (2025), doi:10.1093/emph/eoaf002.

33. J. P. Townsend, *et al.*, Seasonality of endemic COVID-19. *mBio* **14** (6) (2023), doi:10.1128/mbio.01426-23.

34. Z. Grossman, Oscillatory phenomena in a model of infectious diseases. *Theoretical Population Biology* **18** (2), 204–243 (1980), doi:10.1016/0040-5809(80)90050-7.

35. C. Viboud, *et al.*, Synchrony, Waves, and Spatial Hierarchies in the Spread of Influenza. *Science* **312** (5772), 447–451 (2006), doi:10.1126/science.1125237.

36. J. Peccia, *et al.*, Measurement of SARS-CoV-2 RNA in wastewater tracks community infection dynamics. *Nature Biotechnology* **38** (10), 1164–1167 (2020), doi:10.1038/s41587-020-0684-z.

37. M. Morvan, *et al.*, An analysis of 45 large-scale wastewater sites in England to estimate SARS-CoV-2 community prevalence. *Nature Communications* **13** (1) (2022), doi:10.1038/s41467-022-31753-y.

38. U. C. Bureau, County Population Estimates. *Annual Resident Population Estimates, Estimated Components of ResidentPopulation Change, and Rates of the Components of Resident Population Change for States and Counties:April 1, 2020 to July 1, 2022* (2023), accessed March 7, 20224, `https://www.census.gov/data/datasets/time-series/demo/popest/2020s-counties-total.html`.

39. U.S. Census Bureau, National Counties Gazatteer. *U.S. Gazetteer Files* (2023), accessed Septemeber 21, 2023, `https://www.census.gov/geographies/reference-files/time-series/geo/gazetteer-files.html`.

40. MIT Election Data And Science Lab, County Presidential Election Returns 2000-2020 (2018), doi:10.7910/DVN/VOQCHQ.

41. Google LLC, COVID-19 Community Mobility Report (Accessed 2024), https://www.google.com/covid19/mobility.

42. A. Roesch, H. Schmidbauer, *WaveletComp: Computational Wavelet Analysis* (2018), https://CRAN.R-project.org/package=WaveletComp, r package version 1.1.

43. R Core Team, *R: A Language and Environment for Statistical Computing*, R Foundation for Statistical Computing, Vienna, Austria (2024), https://www.R-project.org/.

Acknowledgments

We would like to thank colleagues from the Harvard T.H. Chan School of Public Health, Center for Communicable Disease Dynamics for their helpful and thoughtful discussion and feedback throughout the writing of this paper.

Funding: All authors were supported by the NIH SeroNet cooperative agreement U01CA261277 and I.N.R. was additionally supported by the NIH T32AI007535.

Author contributions: I.N.R. conceived paper and prepared initial draft. I.N.R and W.H. prepared further drafts and all authors contributed to the final draft and provided approval. All authors contributed to model and analysis methodology. I.N.R. and M.B. performed programming and software development. I.N.R created visualizations and performed analyses.

Competing interests: W.P.H. is an advisor to Biobot Analytics, and a consultant to Shionogi Inc.

Data and materials availability: Code for both the spectral analysis and model simulations is available at https://github.com/ilanrubin/COVID-19-Seasonality.